High-energy events, boulder deposits and the use of very high resolution remote sensing in coral reef environments

Antoine Collin†∞, Samuel Etienne‡∞, Serge Planes†∞

†CRIOBE, USR 3278 CNRS-EPHE, BP 1013, 98729, Papetoai, French Polynesia antoinecollin1@gmail.com

‡ Ecole Pratique des Hautes-Etudes, CNRS UMR 8586 Prodig, Laboratory of Coastal Geomorphology and Environment, 15 boulevard de la mer, 35800 Dinard, France samuel.etienne@ephe.sorbonne.fr

∞ Laboratoire d'excellence "CORAIL", France

ABSTRACT

Collin, A., Etienne, S. and Planes, S., 2013. High-energy events, coastal boulder deposits and the use of very high resolution remote sensing. *In:* Conley, D.C., Masselink, G., Russell, P.E. and O'Hare, T.J. (eds.), *Proceedings 12th International Coastal Symposium* (Plymouth, England), *Journal of Coastal Research*, Special Issue No. 65, pp. xxx-xxx, ISSN 0749-0208.

In recent years, coastal boulders have become a trendy proxy in studying high-energy marine inundation events. From their morphology and spatial distribution, authors are able to characterize a singular event in terms of intensity (wave height, flow velocity). Recent post-catastroph studies (e.g. Indian Ocean 2004 and Japan 2011 tsunamis) have demonstrated also the interest of boulder deposits in reconstructing the event kinematics through a multi-proxy approach. But as boulder studies require a statistically robust dataset they are field-time consuming and sometimes fieldwork takes place in remote areas with low facilities. The use of very high resolution remote sensing could overcome some of these limits. In this paper, we evaluate the possibility to identify meter-size coral boulder thrown on a reef flat during the hit of a tropical cyclone. Image analysis allows for the discrimination of major geographical object encountered on coralline islands: submerged coral boulder, emerged coral boulder, perched reef, sand beach. Within emerged boulder population, specific bands available with WorldView-2 images (i.e. red and NIR2 band) allow the spectral discrimination and mapping of fresh and weathered elements.

ADDITIONAL INDEX WORDS: *large clast sedimentology, VHR remote sensing, coral geomorphology, tropical cyclone, French Polynesia.*

INTRODUCTION

Following the Udden-Wentworth scale, a boulder is a clast with intermediate B-axis ranging from -8Φ (256 mm) to -12Φ (4096 mm). Blair and McPherson (1999) have refined this scale by adding 4 grades in the boulder class but discrepancies in the use of this large clast scale are still common and pollutes the scientific debate on the significance of coastal boulder deposits (Paris *et al*., 2011). In coastal environments, boulders emplaced by waves represent a distinct sedimentary class and a signature of high-energy events (cyclones, storms, tsunamis). Until recent years, coastal deposit studies dedicated to boulder assemblages were scarce beside the seminal work by Oak (1984) on boulder beaches. But, after the Indian Ocean tsunami (2004), closer examination of the sedimentary signatures of catastrophic marine inundation enlightened the interest of coarse sediment – in complement with more traditional fine sediment studies – to characterize these events. Nott (1997, 2003) has given a new dimension to boulder studies with the introduction of mathematical modelling of hydrodynamic transport equations. Then, it has become possible to extract quantitative information on flow velocity or wave height from boulder morphometry (Etienne and Paris, 2010). Spatialisation of hydrodynamic information inferred from boulder morphometry offers the opportunity to understand the propagation of catastrophic waves on coastal plains. Boulders have then become a new centre of interest for coastal sedimentologists and boulder deposits appear now as a robust proxy for the reconstruction of high-energy marine inundation events (Etienne *et al*., 2011).

Boulder deposits are naturally remanent objects: they can subsist in the landscapes for decades or centuries (e.g. some tsunami megaclasts emplaced as a consequence of the 1883 Krakatau eruption are still observable in Anyer, Java), except when they are intentionally removed (e.g. Terry and Etienne, 2010). Because of this remanence, it is sometimes difficult to decipher the different generations of boulder deposits, especially in areas where both cyclones and tsunamis are frequent (e.g. Japan: Goto *et al*., 2010). Therefore, a boulder population is often composed of individual elements tied to various cohorts, each cohort corresponding to a single high-energy event, and elements that have been mobilized several times (the probability of multiple mobilisations increasing with age). Dating a clast is sometimes possible for coral reef boulder using radiocarbon or U-series dating of fossils, but it is more difficult for crystalline rocks in the absence of historic documentation (aerial photograph, satellite images, written documents, etc.).

Remote sensing (from spaceborne to airborne imagery) has been widely used for characterizing coastal environments (see Klemas, in press): geomorphology, habitat and resilience mapping, coastal zone management, natural disaster monitoring, etc., but no study has yet focussed on the use of satellite imagery for coastal boulder classification. This can be explained by the pixel resolution limit

which was not in accordance with boulder size which favored the use of digital airborne images (e.g. Compact Airborne Spectrographic Imager). However, very high spatial resolution imagery, delivering data at inframeter resolution, is now available from satellite so that the issue of spectral mixing encountered by lower resolution imagery can be reliably overcome. The present paper provides an insight in the interest of very high resolution (VHR) satellite images (WorldView-2 sensor, WV2) for identifying and classifying coral boulder deposited by tropical cyclone on the reef flat of Tetiaroa atoll, French Polynesia.

STUDY AREA

Tetiaroa is an atoll located in the Society Islands, French Polynesia, in the South Pacific Ocean. In February 2010, the western area of French Polynesia has been hit by Tropical Cyclone (TC) Oli. TC Oli, lasting from 1 to 7 February 2010, was the 5th depressional system, and the 2nd cyclone to occur in the Southwest Pacific basin during the 2009/2010 season. Oli was the first TC to affect French Polynesia Islands in 2010 and the most severe storm since TC Zita and TC Arthur (both category 2 at their peak intensity) which affected the western part of the territory in January 2007. The initial depression developed north of Fiji waters, 3000 km from Tahiti. The system reached category 1 cyclone status (Saffir-Simpson scale) located near 16°S 156.5°W (approximately 700 km west-north west of Tetiaroa, 450 km north of Mauke, Cook Islands) at 6 p.m. local time on 2 February (6 a.m. UTC on 3 February). Twenty-four hours later, TC Oli reached category 2 with sustained winds over 80 knots (150 km/hr) and following a NW-SE track toward Tetiaroa-Tahiti (300 km at its closest). During the night of 3-4 February, the cyclone strengthened rapidly and reached category 4 around midnight (1 min wind speed: 115 knots (210 km/hr)). Its trajectory was then NNW-SSE and impacted directly over Tubuai Island in the Austral archipelago. TC Oli hit this island in the morning of the 5 February (5 p.m. UTC), but wind speed lowered and the cyclone had eased to at category 2. Then the system followed a south-eastern direction, weakened progressively and dissipated 500 km SE of Rapa. The geomorphic impacts of TC Oli have been studied by Etienne (2012). They include submarine reef erosion (coral colony breakage and massive coral colony displacement), fine and coarse sediment transport and beach erosion. Flow velocity variations were estimated through boulder analysis: submarine

boulder measurements provide valuable estimates of flow velocity profile with depth. Beachrock slabs measurements provide also estimates of flow velocities at the reef/beach junction. Combining these different geomorphic markers appeared to be a way to apprehend the flow velocity variation when the cyclone waves cross the coral reef but boulder fieldwork is time consuming and interesting areas might not always be accessible in remote islands.

METHODS

Field Measurements

Coral boulders tossed on the reef flat of Tetiaroa were examined in April 2010, November 2011 and July 2012. Fresh boulders (i.e. emplaced by TC Oli, number of samples n=9) were identified by their whitish appearance and older boulders (n=4) identified by their dark patina or irregular weathered surface (Figure 1). Boulder location (GPS), dimensions (A, B, C axes), orientation of A-axis, and rock characteristics were recorded. On the lagoon-beach contact, contemporary beachrock was often exhumed; beachrock slabs transported inland by the waves (n=5) and fresh scars of missing pavement were measured (n=2). Boulder measurements are used for flow velocity estimation following Nott's (2003) and Nandasena *et al*. (2011) equations (see Etienne, 2012). Added to these clasts, various geographical objects (pier, perched reef flat, *feo*) were located on field using GPS device for satellite image calibration.

Geomorphic Targets

A 3-level classification scheme was designed for the lagoon image analysis (Figure 2). At first level, boulders are isolated from coralligeneous sand and perched reef. Then, at second level,
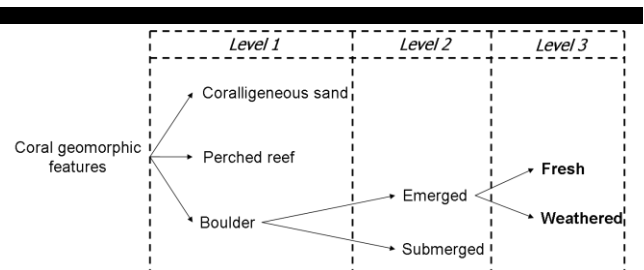

Figure 2. Classification scheme of the investigated coral geomorphic features dividing into three levels of precision.

submerged boulders (i.e. living coral colonies) are isolated from emerged boulders (i.e. dead coral colonies). Finally, at third level, fresh (white) boulders emplaced by TC Oli are distinguished from weathered boulders associated with older high energy events.

Image Analysis

Remote sensing imagery allows for the generation of thematic maps based on image classification. Even though the airborne sensors show spectral and spatial capabilities for surveying boulders at appropriate scales, they suffer from a poor data/time collection ratio and are greatly reliant on several hours of favorable weather conditions. Conversely, data from spaceborne remote sensing are acquired over dozens of km^2 in a snapshot and now benefits from the inframeter scale since the WV2 inception. WV2 imagery is composed of eight 2 m multispectral bands, ranging from 400 to 1040 nm, and one 0.5 m panchromatic band, spanning a gamut of 450-800 nm. Tetiaroa imagery was acquired on 14 October 2010 in the form of two datasets. No high-energy

Figure 1. Coral boulder field on the reef flat of Tetiaroa atoll, French Polynesia. Coral colonies overturned by Tropical Cyclone Oli in February 2010 appear in white whereas older boulders have a dark appearance due to the development of a biological patina and weathering processes. Picture: April 2010.

or major pollution event occurred between the imagery acquisition and the TC Oli impact. Prior identifying boulders, pre-processing steps were carried out to fully exploit standardized data. For each dataset, a pansharpening procedure was completed in order to handle eight 0.5 m multispectral bands (cf. Collin *et al.* 2012 for
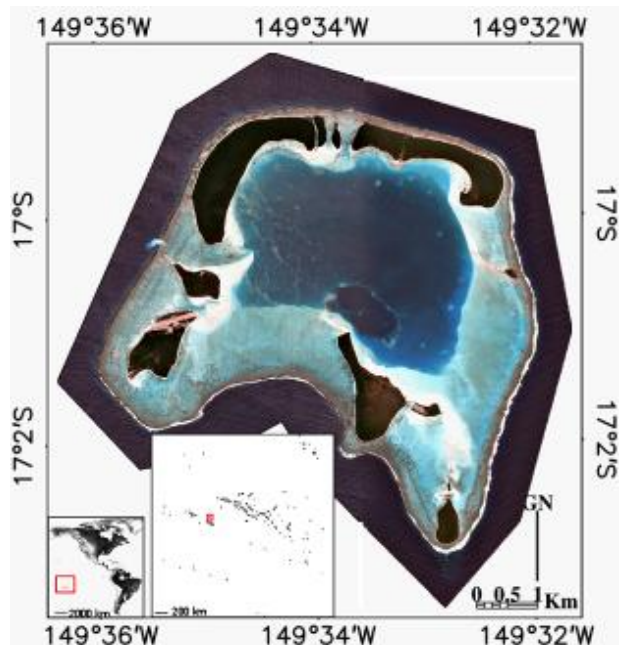

Figure 3. Natural-colored (RGB: 532) image of Tetiaroa atoll, French Polynesia. The value of image pixels represents the orthorectified water-leaving reflectance.

further details). Geometric and atmospheric correction were then applied, using the specifically dedicated modules within the IDL-ENVI software (Research Systems Inc., 2005), so that both datasets of water-leaving reflectance can be rigorously mosaicked (Figure 3).

Linking real-world coral geomorphic features with remotely-sensed imagery was achieved by means of the method of region of interest (ROI). Based on the surveyed geolocated features and the spatial consistency that can be directly grasped from georeferenced imagery, ROI related to geomorphic classes included into the three levels (cf. Figure 2) were spatially seeded over the exact field-imagery geographic correspondence and cautiously grown until reaching obvious, closest boundaries. Thus, for each of the five leaf classes and the two node classes (cf. Figure 2), eight spectral data per pixel were retrieved from WV2 imagery and then averaged across constitutive pixels so that a spectral signature can be assigned to each class. Standard errors were calculated and associated with averages in the curve plots to visually capture the separability among them. Given the conveyed insight in terms of temporal occurrence, the discrimination between the two classes of the level 3, reflecting two weathering stages, was further examined in computing a *Z*-test for the eight spectral comparisons (Figure 4). Using standard statistical methods, and assuming a normal distribution of residuals, a *Z*-test standardizes a sample distribution (using means and variances of the two datasets) to a normal distribution, and is a test of statistical significance helping whether or not rejecting the null hypothesis. The null hypothesis for our case states that there is no difference among the values associated with the two datasets. A *Z*-test greater than $|1.96|$ shows a significant difference between the two

datasets (*p-value*<0.05 or 95% confidence level), while a *Z*-test less than $|1.96|$ indicates an insignificant difference between them. The NDVI (Normalized Difference Vegetation Index) is used to transform multispectral data into a single image band representing vegetation distribution (Tucker, 1979), highly valuable for monitoring natural land disaster (Martino *et al.*, 2009). NDVI standard algorithm is the difference between the near-infrared (highly reflected by chlorophyll vegetation) and red (highly
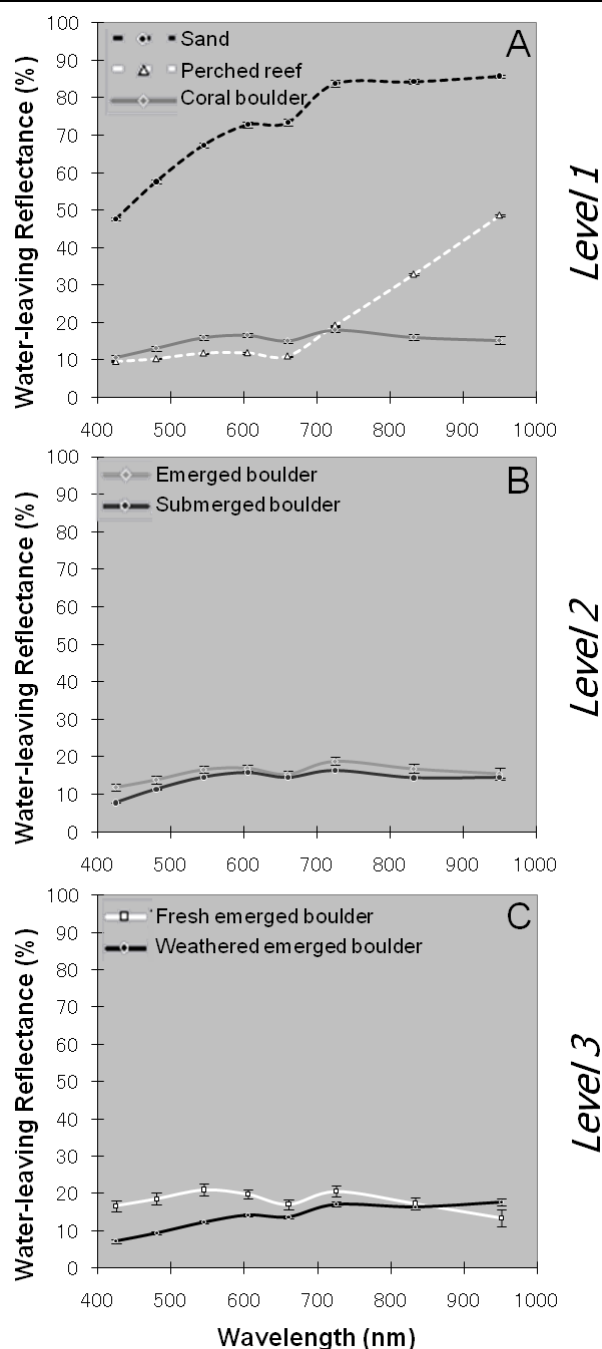

Figure 4. Curve plots of the spectral signatures of the seven coral geomorphic features based on WorldView-2 measurements. The geomorphic features are plotted against the precision level, from the coarser to the finer: level 1 (A), level 2 (B), and level 3 (C).

Table 1. Coral boulder reflectance (%) signatures and associated *Z*-tests derived from a WorldView-2 imagery collected over Tetiaroa, French Polynesia. Count: weathered boulder n=171; fresh boulder n=25. The threshold of the statistical significancy is fixed at p<0.05.

WV2 band	425	480	545	605	660	725	832.5	950
Mean reflectance								
Weathered	7.16	9.31	12.28	14.23	13.73	17.12	16.44	17.73
Fresh	16.72	18.57	21.04	19.82	17.04	20.58	17.26	13.33
Standard error								
Weathered	0.48	0.43	0.43	0.36	0.43	0.62	0.87	0.90
Fresh	1.47	1.63	1.66	1.32	1.34	1.46	1.60	2.23
Z-test	-6.19	-5.48	-5.11	-4.08	-2.36	-2.18	-0.45	1.83
Significance	*p*<0.001	*p*<0.001	*p*<0.001	*p*<0.001	*p*<0.001	*p*<0.001	Non-Significant	Non-Significant

Table 2. Five coral geomorphic features NDVI values and associated *Z*-tests derived from WorldView-2 red, "red edge", NIR1 and NIR2 channels. Count: sand n= 2013; perched reef n=1245; submerged reef n=528; fresh boulder n=25; weathered boulder n=171. Underlined *Z*-tests indicate the non-significance of the difference between the pairwise NDVI values, while the non-underlined *Z*-tests indicate the significance of the difference between them (p<0.05).

	Perched reef			**Submerged boulder**			**Fresh boulder**			**Weathered boulder**		
	red-"red edge"	*red-NIR1*	*red-NIR2*	*red-"red edge"*	*red-NIR1*	*red-NIR2*	*red-"red edge"*	*red-NIR1*	*red-NIR2*	*red-"red edge"*	*red-NIR1*	*red-NIR2*
Sand	-45.45	-87.97	-91.76	53.64	167.5	181.8	<u>-1.88</u>	3.72	5.31	<u>-0.87</u>	3.87	3.39
Perched reef				73.39	266.1	445.6	13.61	18.87	12.95	13.04	18.62	18.33
Submerged boulder							-12.65	-20.08	-8.43	-10.50	-19.29	-23.46
Fresh boulder										<u>0.61</u>	<u>0.18</u>	-3.18

absorbed by chlorophyll vegetation) bands divided by the sum of these two bands. The higher the NDVI the higher the chlorophyll content of the selected pixel or ROI.

$$NDVI = \frac{R_{NIR} - R_{red}}{R_{NIR} + R_{red}} \qquad (1)$$

with R_{NIR} and R_{red} refer to reflectance of the near-infrared (WV2 band 6, 7 and 8, called "red edge", NIR 1 and NIR 2, respectively) and red (WV2 band 5) spectral bands.

We have used the NDVI as an attempt to provide a spectral proxy aiming at deciphering the various geomorphic features at stake in a simply-designed, and -implemented manner to rapidly serve scientists and managers tasked with coastal disasters. Still adopting the ROI approach, we have compared the five leaf classes using the *Z*-test, and chosen the NDVI furnishing the best discrimination among geomorphic features (Figure 5). We have therefore been able to spatially model it over the whole area at a 0.5 m spatial resolution in the form of a Digital NDVI Model (DNDVIM)(Figure 6).

Beyond the spectral composition of the geomorphic targets, the two-dimensional (projected) topology of the emerged coral boulders has been investigated using the DNDVIM. We retrieved the dimensions (A and B axes) and the orientation of the A-axis of the most massive coral boulders. This set of data can be compared with direct field measurements.

PRELIMINARY RESULTS AND DISCUSSION

With the objective of discriminating emerged boulders from perched reef (*feo*), we have presumed that higher degrees of weathering and biofilm incrustation on perched reef would deliver a higher NDVI index. The red-NIR2 NDVI values of the fresh boulder (negative) were significantly lower to those of the weathered boulder, which were close to 0. We can deduce that the NIR2 reflectance values were lower than those of the red for the fresh boulder and mostly equal for the weathered boulder. Three hypotheses can be proposed to explain the difference: (1) an increase in NIR2 reflectance, (2) a decrease in red reflectance, (3) the combined latter conjectures. According to the results in Table 1 showing the thorough balance between NIR2 gain and red loss in reflectance (gain of 4% in the NIR2 reflectance and loss of 4% in red reflectance), the combination hypothesis thereby exhibits the greatest explanatory power. The spectral shift occurring from a fresh to weathered boulder may be intricately linked with the ontogenetic colonization of the surface by photosynthetic micro-organisms, endowed with chloroplasts absorbing the red and reflecting the NIR radiation (Gross, 1991).

Discrepancies in NDVI values occurred over the mosaic around a vertical axis at approximately 149 ^{o} 33'5''W. This manifest boundary is likely to result from the mosaicking process merging one western and one eastern image (Figure 7). Insofar as the western image showed spectral speckles due to wind-driven sea surface rugosity, the reflectance in the NIR2 was skewed. Instead of being substantially absorbed by water, radiation in NIR2 was reflected by water due to the rugosity, leading to fallaciously increase the NDVI. We therefore advocate applying a glint removal procedure (Hedley *et al.* 2005) on images obviously affected by sea surface rugosity before computing the NDVI, and before, if any, mosaicking images.
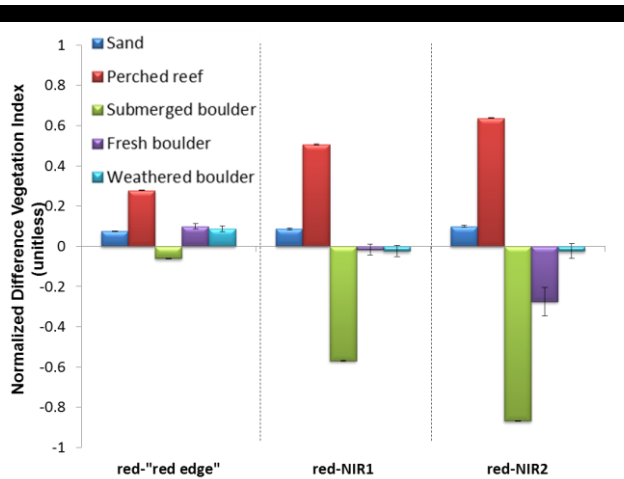
Figure 5. Bar plots of Normalized Difference Vegetation Indices (NDVI) of the five leaf classes of the geomorphic features in respect of the WorldView-2 infrared bands ("red edge", NIR1 and NIR2). Coloured bars are means and black bar errors represent standard errors.

Except NIR1 and NIR2, six other WV2 bands enabled to significantly distinguish between fresh and weathered boulder (Table 1). Unlike the NDVI built with "red edge" and NIR1 (and red), the NDVI derived from NIR2 has the potential to significantly discriminate the five leaf classes of the geomorphic features (Table 2). Beyond the feasibility of the spectral discrimination, other boulder characteristics are of particular interests in remote sensing: classes based on the position and the orientation. But a strong limitation is that only A and B axes are measurable with a single satellite image whereas C axis is necessary for boulder volume calculation. This third dimension of the topology might be achieved through VHR stereophotogrammetry.

Table 3. Comparison of boulder dimensions acquired during fieldwork and extracted from WorldView-2 images. A, B: length and width measured in situ; A', B': length and width extracted.

Boulder	Field	(cm)	WV2	(cm)	Error	(%)
	A	B	A'	B'	Δ (AA')	Δ (BB')
1	342	278	302	240	11.7	13.7
2	180	175	200	137	11.1	21.7
3	200	200	187	185	6.5	7.5
4	180	100	159	152	11.7	52.0
5	190	160	175	175	7.9	9.4
6	230	170	274	202	19.1	18.8
7	280	226	230	212	17.9	6.2
8	645	260	638	280	1.1	7.7
9	84	60	100	87	19.0	45.0
10	215	200	188	150	12.6	25.0
11	790	430	682	454	13.7	5.6
12	480	340	508	378	5.8	11.2
13	200	140	215	142	7.5	1.4
mean	**309**	**211**	**297**	**215**		

NB: Δ (AA')=|(A−A')/A'| and Δ (BB')=|(B−B')/B'|
Coral boulders selected for field measurement have a mean long-axis (A) equals to 3.1 m and an intermediate axis (B) equals to 2.1 m. Their horizontal surface covers 0.5 to 34 m² (mean = 8.2) which represents 1 to 120 full pixels in panchromatic mode. Data extracted from images give a mean A' axis equals to 3.0 m and a

mean B' axis equals to 2.1 m (Table 3). Error (i.e. standardized variation) between in situ measurements and extracted dimensions are under 20% for any dimension >1.5 m, and under 15% for any dimension >2.8 m. Smallest boulders (axis<1.5 m) are difficult to measure precisely due to image resolution limit.
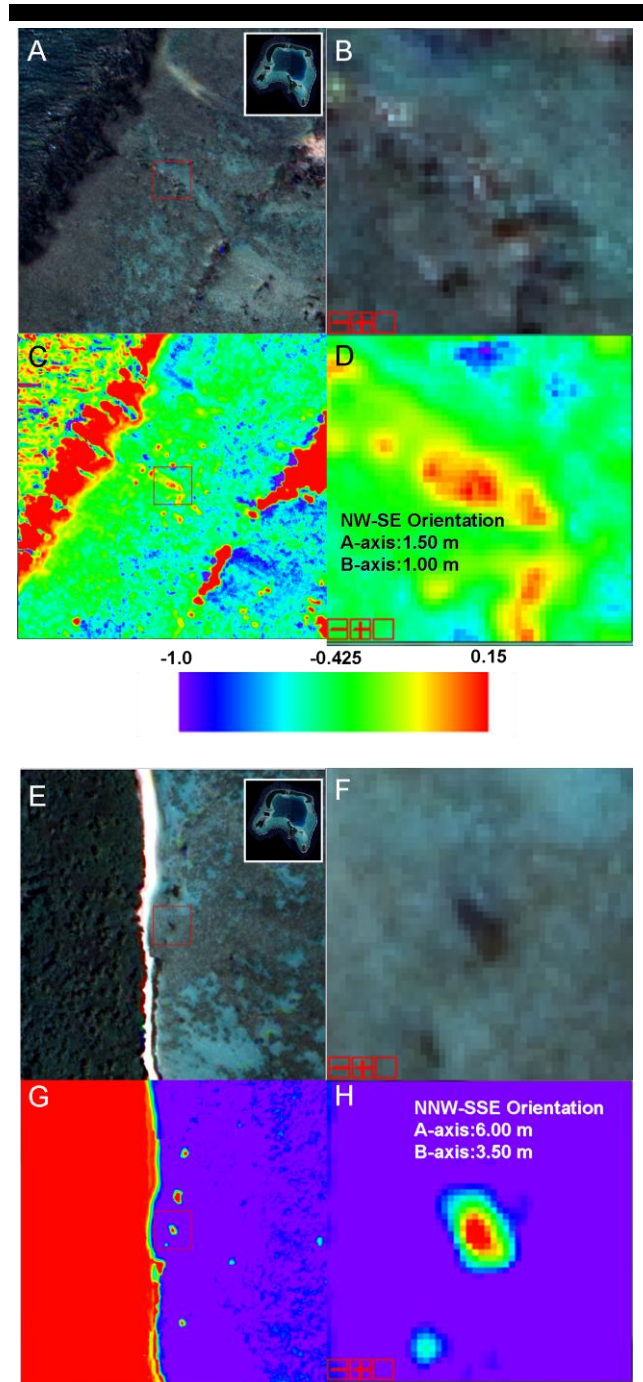

Figure 6. The spatial detection of the targeted fresh boulder and weathered boulder in the form of the WorldView-2 true-coloured representation (scroll-image and zoom: A, B; and E, F, respectively) and the WorldView-2 red-NIR2 DNDVIM (image and zoom: C, D; and G, H, respectively). Dimensions (A- and B-axes) of the two targets are retrieved straightforwardly from the DNDVIM.
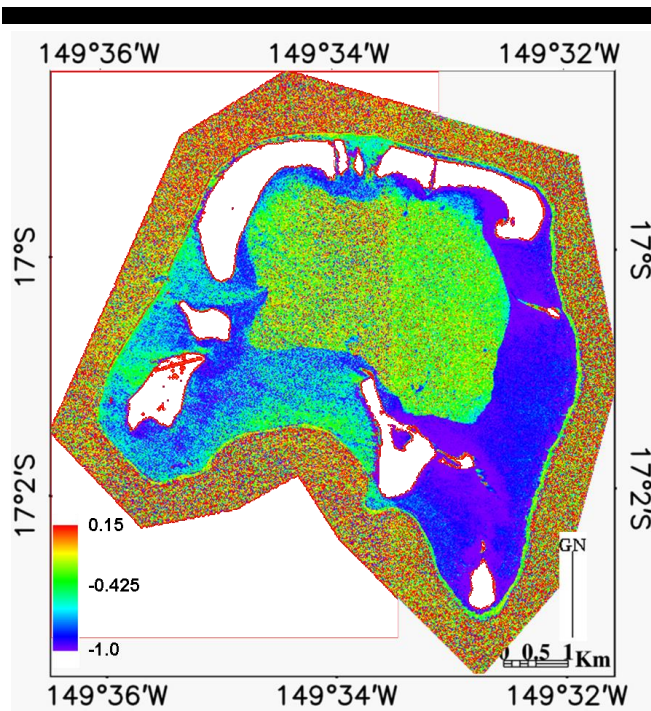
Figure 7. Rainbow-coloured Digital Normalized Difference Vegetation Index Model (DNDVIM) based on the WorldView-2 red and NIR2 channels.

CONCLUSION

Boulder studies are more and more numerous in coastal geomorphology. Boulder deposits appear as a robust proxy for high-energy marine inundation studies but data collection or boulder localization are sometimes difficult, especially in remote oceanic islands. Very high resolution remote sensing offers new opportunities to study small-size object like meter-size boulders. Image analysis allows for the discrimination of major geographical object encountered on coralline islands: submerged coral boulder, emerged coral boulder, perched reef, sand beach. Within emerged boulder population, specific bands available with WorldView-2 images (i.e. red and NIR2 band) allow the spectral discrimination and mapping of fresh and weathered elements. Precise measurements of long and mean intermediate axis are also possible with a small error for objects >2 m. This tool should be better considered for coastal boulder deposit mapping including pluri-annual monitoring purpose or post-catastrophic marine submersion survey.

ACKNOWLEDGEMENT

LITERATURE CITED

Blair, T.C., McPherson, J.G., 1999. Grain-size and textural classification of coarse sedimentary particles. *Journal of Sedimentary Research*, 69, 6-19.

Collin, A., Roelfsema, C., Archambault, P., Planes, S., 2012. Seamless bridging of land-to-coral reed coastal patches through very high resolution mapping, PLoS One, submitted.

Etienne, S., 2012. Marine inundation hazards in French Polynesia: geomorphic impacts of Tropical Cyclone Oli in February 2010. *The Geological Society of London*, Special Publications, 361, 21-39.

Etienne, S., Buckley, M., Paris, R., Nandasena, A.K., Clark, K., Chagué-Goff, C., Goff, J., Richmond, B., 2011. The use of boulders for characterizing past tsunamis: lessons from the 2004 Indian Ocean and 2009 South Pacific tsunamis. *Earth-Science Reviews*, 107, 75-90.

Etienne, S., Paris, R., 2010. Boulder accumulations related to storms on the south coast of the Reykjanes Peninsula (Iceland). *Geomorphology*, 114, 55-70.

Goto, K., Kawana, T., and Imamura, F., 2010. Historical and geological evidence of boulders deposited by tsunamis, southern Ryukyu Islands, Japan. *Earth-Science Reviews*, 102, 77-99.

Gross, J., 1991. Pigments in vegetables. Chlorophylls and carotenoids. Avi:Van Nostrand Reinhold Company Inc, New York.

Hedley. J. D., Harborne, A.R., Mumby, P. J., 2005. Technical note: Simple and robust removal of sun glint for mapping shallow-water benthos. *International Journal of Remote Sensing*, 26(10), 2107-2112.

Klemas, V. in press. Airborne remote sensing of coastal features and processes: an overview. *Journal of Coastal Research*. DOI: 10.2112/JCOASTRES-D-12-00107.1

Marshall, M.T., Funk, C., and Michaelsen, J., 2012. Agricultural drought monitoring in Kenya using evapotranspiration derived from remote sensing and reanalysis data. *In:* Wardlow, B.D., Anderson, M.C., and Verdin, J.P. (eds). *Remote sensing of drought. Innovative monitoring approaches*. Boca Raton: CRC Press, Taylor & Francis, pp.169-193.

Martino, L., Ulivieri, C., Jahjah, M., and Loret, E., 2009. Remote Sensing and GIS Techniques for Natural Disaster Monitoring. *In:* Olla, P. (ed.). *Space Technologies for the Benefit of Human Society and Earth*, Springer, pp. 331-382.

Nandasena, N.A.K., Paris, R., and Tanaka, N., 2011. Reassessment of hydrodynamic equations: Minimum flow velocity to initiate boulder transport by high energy events (storms, tsunamis). *Marine Geology*, 281, 70-84.

Nott, J. 1997. Extremely high-energy wave deposits inside the Great Barrier Reef, Australia: determining the cause- tsunami or tropical cyclone. *Marine Geology*, 41, 193-207.

Nott, J., 2003. Waves, coastal boulder deposits and the importance of the pre-transport setting. *Earth and Planetary Science Letters*, 210, 269-276.

Oak, L.H., 1984. The boulder beach: a fundamentally distinct sedimentary assemblage. *Annals of the Association of American Geographers,* 74, 71-82.

Paris, R., Naylor, L.A., and Stephenson W.J., 2011. Boulders as a signature of storms on rock coasts. *Marine Geology*, 283, 1-11.

Terry, J.P., Etienne, S., 2010. "Stones from the dangerous winds": reef platform mega-clasts in the tropical Pacific Islands. *Natural Hazards*, 56, 567-569.

Tucker, C.J., 1979. Red and photographic infrared linear combinations for monitoring vegetation. *Remote Sensing of Environment*, 8 (1979), 127–150.